

Low temperature synthesis of mesoporous CaFe_2O_4 photocathodes with hierarchical pore morphology

Kristin Kirchberg^a, Roland Marschall^{b,*}

^aInstitute of Physical Chemistry, Justus-Liebig-University, Heinrich-Buff-Ring 17, 35392 Giessen, Germany

^bChair of Physical Chemistry III, University of Bayreuth, Universitätsstrasse 30, 95447 Bayreuth, Germany

Experimental Details

Synthesis: Classical sol-gel synthesis of phase-pure, porous CaFe_2O_4 thin films was achieved by adaption of a procedure reported for mesoporous ZnFe_2O_4 thin films.^[1] The synthesis pathway is depicted in **Figure S1**. More precisely, 132.3 mg of $\text{Ca}(\text{NO}_3)_2 \cdot 4 \text{H}_2\text{O}$ (0.56 mmol, 99.98 %, ALFA AESAR), 348.3 mg $\text{Fe}(\text{NO}_3)_3 \cdot 9 \text{H}_2\text{O}$ (0.862 mmol, 99.99 %, SIGMA ALDRICH) and 45 mg of block-copolymer poly(ethylene oxide)-*b*-poly(propylene oxide)-*b*-poly(ethylene oxide) (Pluronic® F-127, abbr. PLU, SIGMA ALDRICH) were dissolved in 1.7 mL of ethanol (> 99.8 %, ACROS) and 0.6 mL of 2-methoxyethanol (> 99.3 %, ABCR) by ultrasonic treatment. A 30 wt% excess of calcium precursor was used, as calcium nitrate is highly hygroscopic and was found to not yield in phase-pure CaFe_2O_4 when stoichiometric amounts were used. The clear, intense red solution was filtered through a syringe filter (PTFE, 0.2 μm) into a dip coating vessel. The vessel was placed inside a dip coating chamber with a controlled humidity of 10 – 15 %. Dip coating of silicon (100) wafers (SILTRONIC) and indium tin oxide (ITO) coated quartz glass slides (PRÄZISIONS GLAS & OPTIK) was performed with a constant speed of 8 mm s^{-1} . The as-coated substrates were pre-dried inside the

dip coating chamber for 3 min and then transferred into a muffle furnace (NABERTHERM), which was pre-heated to 130 °C. With polymer soft template Pluronic® F-127, which forms spherical micelles in solution, an evaporation induced self-assembly (EISA) during the withdrawal step leads to finely distributed polymer micelles within the formed precursor sol. After three hours, the temperature was increased to 300 °C with a heating rate of 0.5 °C min⁻¹ for sol-gel transition. Afterwards, the gel thin films were calcined with holding times of either 1 hour at 700 °C, 4 hours at 700 °C or 12 hours at 600 °C, respectively, for complete polymer removal and transformation into porous CaFe₂O₄.

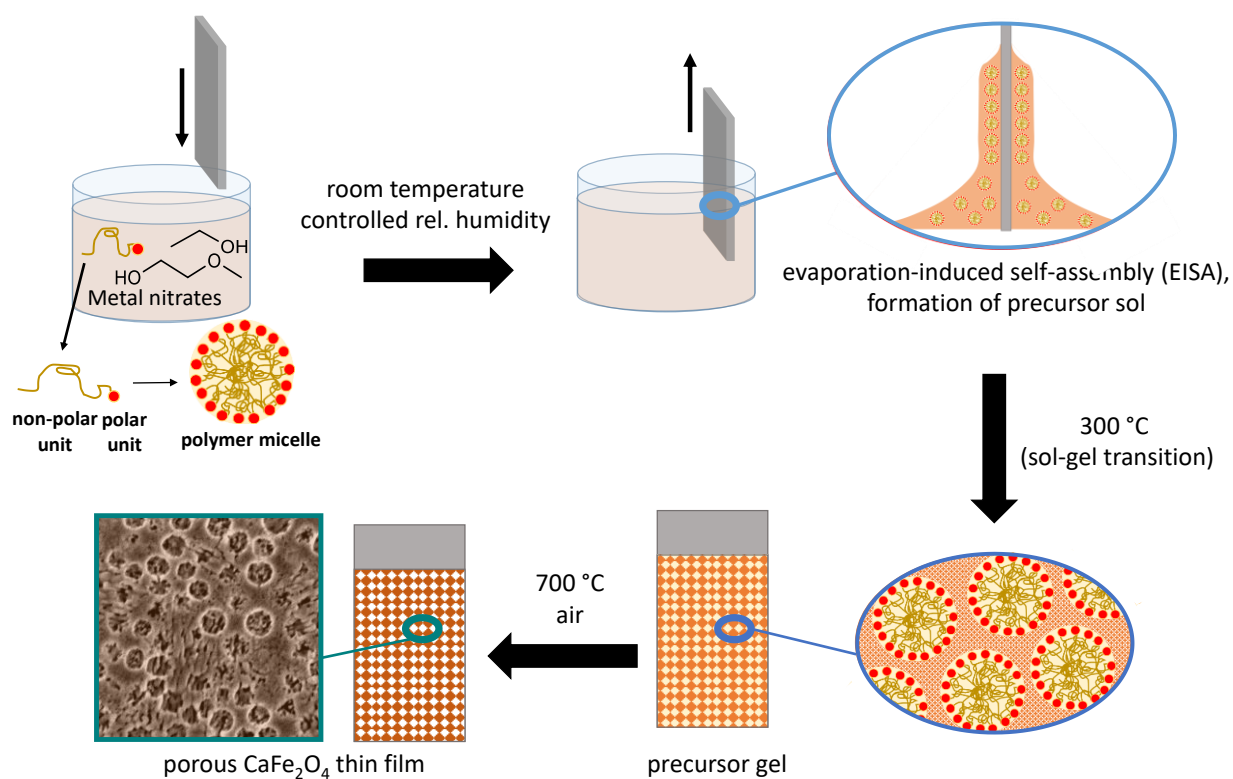


Figure S1. Synthesis procedure for porous CaFe₂O₄ thin films.

Characterisation

Grating incidence X-ray diffraction (GIXRD) patterns of the prepared thin films were collected on an *X'Pert Pro MRD* (PANalytical) equipped with a parallel plate collimator (0.27°) and Cu W/Si mirror applying an Emyrean Cu LFF HR X-ray tube (Cu K α radiation, $\lambda = 1.5406 \text{ \AA}$). For all measurements, a 1.4 mm anti-scatter slit, a 0.04 rad soller slit, a 1/16° divergence slit and a 2 mm mask were mounted. Patterns were recorded with an emission current of 40 mA and an acceleration voltage of 40 kV. For *in situ* measurements at elevated temperatures in synthetic air (80 % N₂, 20 % O₂), a domed hot stage (*DHS 1100*, ANTON PAAR) was used and samples were heated to the desired temperatures with a heating rate of 10 °C min⁻¹.

The Scherrer equation (equation (1)) was used for estimation of the crystallite size. For this purpose, three reflections ((200), (311), (220)) were fitted with a Gaussian curve and the average of the obtained crystallite sizes was taken.

$$L_a = \frac{K \cdot \lambda}{FWHM \cdot \cos \Theta} \quad (1)$$

with L_a (average crystallite size), $FWHM$ (full width at half maximum), K (Bragg constant (0.93)), Θ (Bragg angle), λ (wavelength of X-ray radiation).

Raman spectra of all samples were measured on a BRUKER *Senterra* Raman microscope. Sample excitation was realized with a Nd:YAG laser ($\lambda = 532 \text{ nm}$) at a laser power of 2 mW. 50x magnification and a spectral resolution of 9 – 12 cm⁻¹ were chosen. In general, 40 co-additions and 20 seconds integration time were used. The obtained spectra were processed using *OPUS 7.5* software (BRUKER). The Si substrate Raman signal was subtracted from the data obtained for samples coated on silicon wafers.

Fourier transformed infrared spectra (FTIR) of the polymer template, the precursor sol and the precursor gel were collected on an *IFS25 FTIR spectrometer* (BRUKER). For this purpose, the precursor solution was dried and heat treated at either 130 °C or 300 °C to form the sol or gel, respectively. The obtained powder

samples were pressed with KBr to obtain pellets, which were analyzed between 400 and 4000 cm^{-1} with a step width of 4 cm^{-1} .

Thermogravimetric analyses (TGA) of the precursor sol was realized with a *STA409PC* thermo-scale (NETZSCH) equipped with a *QMG421* quadrupole mass spectrometer (MS, 70 eV ionization energy, BALZERS). The dried powder samples were heated from 30 °C to 800 °C with a heating rate of 5 °C min^{-1} in synthetic air (80 % N_2 , 20 % O_2), while the mass loss and typical MS signals were detected.

The obtained thin films were analyzed with a *MERLIN* field emission scanning electron microscope (FE-SEM, ZEISS) to obtain SEM images. An accelerating voltage of 3 keV, a sample current of 90 pA and a working distance of 2.5 ± 1 mm were chosen for optimum analysis conditions. Additionally, energy-dispersive X-ray (EDX) spectra were detected employing an *X-Max 50* energy dispersive X-ray spectroscopy analyzer (OXFORD INSTRUMENTS) at an accelerating voltage of 10 keV, a sample current of 1000 pA and a working distance of 5 mm.

X-ray photoelectron spectroscopy (XPS) was performed on *PHI Versaprobe II Scanning ESCA Microprobe* (PHYSICAL ELECTRONICS) equipped with an Al $\text{K}\alpha$ X-ray source. The X-ray beam had a size of 0.1 x 1.3 mm and a power of 50 W. Detailed spectra were recorded at an analyzer pass energy 23.5 eV with a step size of 0.2 eV and a step time of 50 ms. The binding energies of all measured samples were referenced by setting the main adventitious carbon C 1s peak, which results from C-C and C-H surface bonds, to 284.8 eV.^[2] All data was processed using *CasaXPS* software (CASA SOFTWARE).

An *AUTOSORB-iQ* setup (QUANTACHROME) was used for krypton physisorption measurements at 77 K. The thin films coated on Si wafers were degassed prior to the physisorption measurements at 300 °C for 5 hours. Data was processed using *ASiQWin* software (Version 4.0, QUANTACHROME) using the BET model for surface area determination with a cross section of 0.205 nm^2 per Kr atom.

CaFe₂O₄ thin films deposited on ITO-coated quartz glass slides were analyzed *via* ultraviolet-visible light (UV-Vis) spectroscopy on a *Lambda 750 UV/Vis-NIR* spectrometer (PERKIN ELMER) in transmission (TR) mode from 800 nm to 250 nm with a step width of 1 nm.

Photoelectrochemical Characterization

All photoelectrochemical measurements were performed on a ZAHNER *Zennium* potentiostat using a three electrode combination (Pt counter electrode, Ag/AgCl in 3 M NaCl reference electrode). Samples were mounted as working electrodes in a PTFE cell with quartz glass window (ZAHNER) and the illuminated area was fixed to 1 cm². A 0.1 M Na₂SO₄ electrolyte solution was purged with argon prior to the measurements (pH = 6.7, CaFe₂O₄ is stable down to pH 4). On the one hand, the electrolyte was used as prepared, and on the other hand suitable sacrificial agents were added. In the first case, 10 % of methanol was added to the electrolyte, whereas the electrolyte was mixed with hydrogen peroxide (H₂O₂) in the second case, resulting in a H₂O₂ concentration of 12.2 mM (pH = 7.2).

Mott Schottky measurements were performed in the dark with a potential sweep of 10 mV /s⁻¹ measuring from 0.2 V_{RHE} to 1.4 V_{RHE} at 100 Hz frequency with 5 mV amplitude. Flat band potentials and donor densities were calculated using the Mott Schottky equation and the relative permittivity of the material ($\epsilon_r(\text{CaFe}_2\text{O}_4) = 10$).^[3] For photocurrent under discontinuous irradiation, one sun illumination was used employing a Xe arc light source (300 W, LOT-QUANTUMDESIGN) equipped with an AM 1.5 G filter operated in a distance of 16 cm from the working electrode surface. IPCE measurements at 0.1 V and 100 mHz were conducted in the presence and also in the absence of suitable sacrificial agents under front side illumination between 292 nm and 593 nm using the TLS unit from ZAHNER.

Flatband potentials and acceptor densities of the synthesized photoelectrodes were calculated on the basis of the Mott Schottky equation according to equation 2 and 3.

$$U_{\text{FB}} = \frac{-b}{m} \quad (2)$$

$$N_{\text{A}} = \frac{2}{e \cdot \epsilon_{\text{r}} \cdot \epsilon_0 \cdot A \cdot m} \quad (3)$$

with U_{FB} (flatband potential), N_{A} (acceptor density), b (intersection with y axis of the linear part of Mott Schottky plot), ϵ_{r} (permittivity of CaFe_2O_4 (287)^[4]), m (slope of the linear part of the Mott Schottky plot), A (analyzed area (1 cm^2)), e (elementary charge), ϵ_0 (permittivity of vacuum). For calculation of the charge injection and charge separation efficiencies, equations 4 and 5 were applied according to a procedure reported by Dotan *et al.*^[5] J_{abs} was chosen as 16 mA/cm^2 according to Li *et al.*^[6]

$$J_{\text{H}_2\text{O}} = J_{\text{abs}} \cdot P_{\text{sep}} \cdot P_{\text{inj}} \quad (4)$$

$$J_{\text{H}_2\text{O}_2} = J_{\text{abs}} \cdot P_{\text{sep}} \quad (5)$$

with $J_{\text{H}_2\text{O}}$ (photocurrent density in water), P_{sep} (charge separation efficiency), $J_{\text{H}_2\text{O}_2}$ (photocurrent density with H_2O_2 sacrificial agent), P_{inj} (charge injection efficiency), J_{abs} (total photocurrent density due to absorbed photons).

Supporting Data

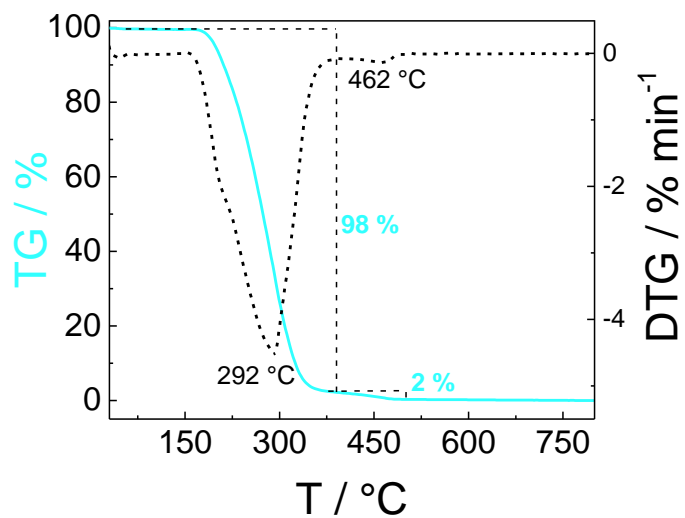


Figure S2. TG-DTG curves of the thermal decomposition of Pluronic® F-127 in synthetic air.

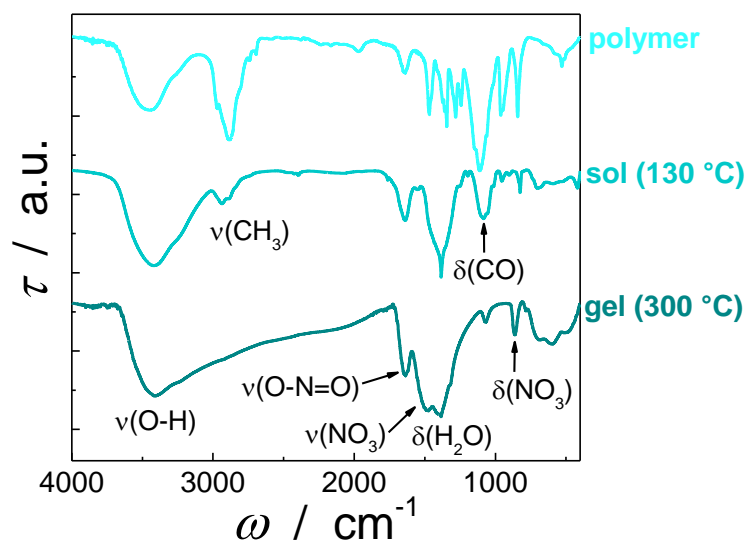


Figure S3. IR pattern of Pluronic® F 127, the precursor sol and the precursor gel.

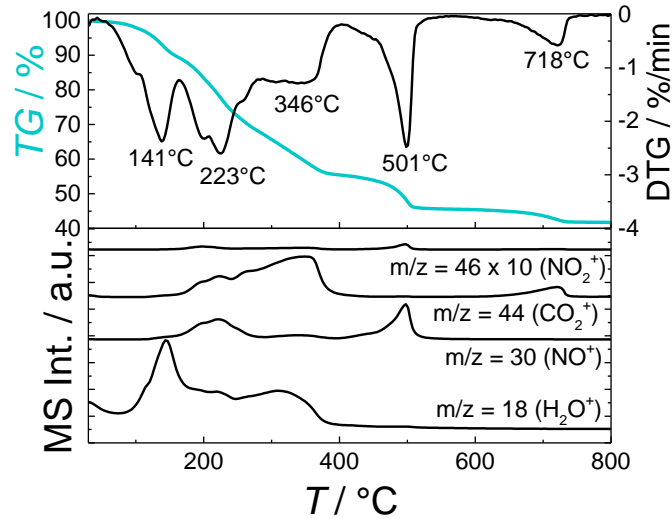


Figure S4. TG and DTG data (upper graph) and MS traces (lower graph) for the calcination of the precursor sol.

The weight loss at 141 °C was assigned to crystal water (H_2O^+ fragment, $m/z = 18$), followed by partial removal of the nitrate building blocks and the polymer template at 223 °C and 346 °C indicated by the MS signals of NO^+ ($m/z = 30$), NO_2^+ ($m/z = 46$) and CO_2^+ ($m/z = 44$). A defined weight loss at 501 °C was assigned to decomposition of the nitrate precursor units. The final decomposition step at 718 °C is accompanied by a CO_2^+ MS signal, which could either result from removal of carbon residues generated during polymer pyrolysis or from decomposition of CaCO_3 , which was formed during the synthesis.

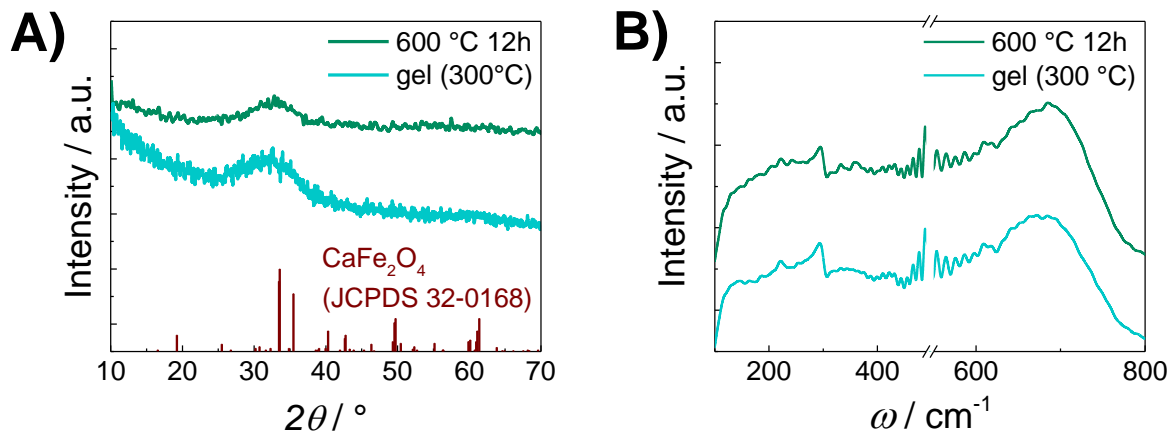


Figure S5. A) GIXRD patterns and B) Raman spectra of samples and obtained after calcination at 300 °C and 600 °C.

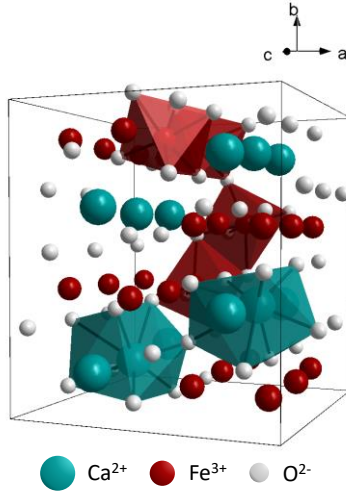


Figure S6. Crystal structure of orthorhombic CaFe₂O₄.

Table S1. Raman signals of CaFe₂O₄ thin films compared to literature values.

CaFe ₂ O ₄ 700 °C 1h (on Si @ 300 K)	CaFe ₂ O ₄ 700 °C 4h (on Si @ 300 K)	CaFe ₂ O ₄ single crystal ⁷ mode (wavenumber)	Ca ₂ Fe ₂ O ₅ ground single crystal ⁸ mode (wavenumber)
119	120	A _g (121)	-
159	146	B _{2g} (155)	-
176	180	B _{2g} (183)	-
203	205	A _g (210)	-
217	222	B _{2g} (224)	-
-	244	A _g (249)	A _g (251)
269	272	A _g (267)	A _g (261)
288	292	A _g (290)	A _g (292)
-	308	B _{2g} (298)	A _g (313)
337	341	B _{2g} (337)	-
363	364	B _{1g} or B _{3g} (367)	-
-	377	A _g (371)	A _g (380)
400	406	A _g (406)	A _g (393)
439	437	A _g (428) or B _{2g} (431)	A _g (428)
-	451	A _g (451)	-
582	580	A _g (578) or B _{2g} (588)	A _g (595)
643	646	A _g (658)	-
-	716	-	A _g (709)

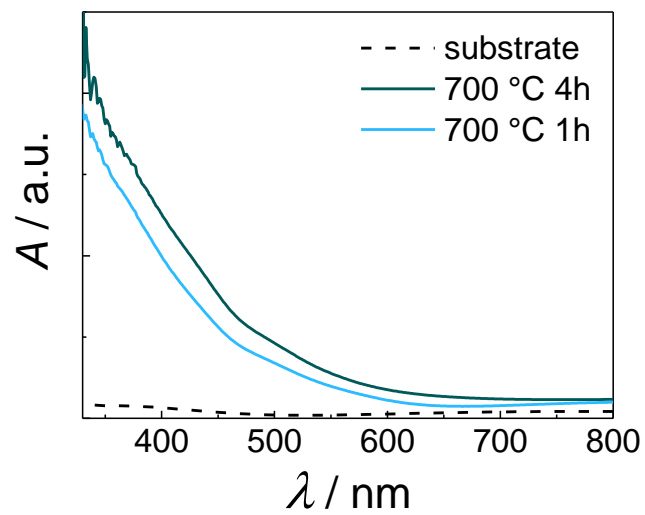


Figure S7. UV-Vis absorption spectra of CaFe_2O_4 thin films on ITO-coated quartz glass.

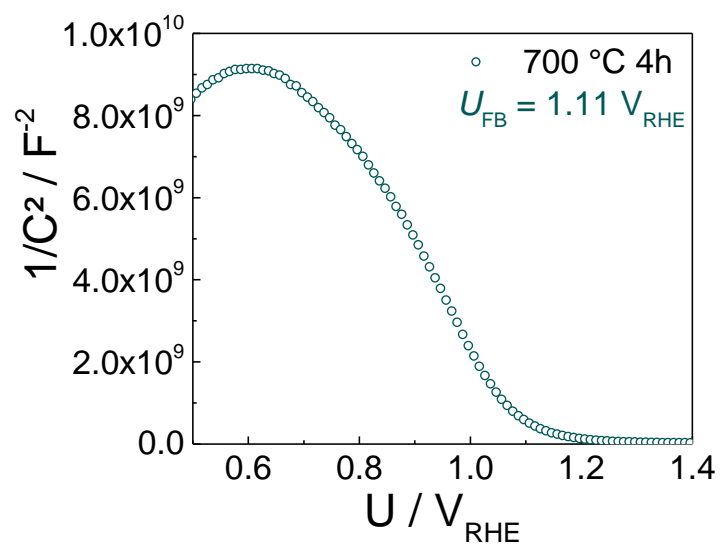


Figure S8. Mott Schottky plot of a CaFe_2O_4 photoelectrode calcined for 4 hours.

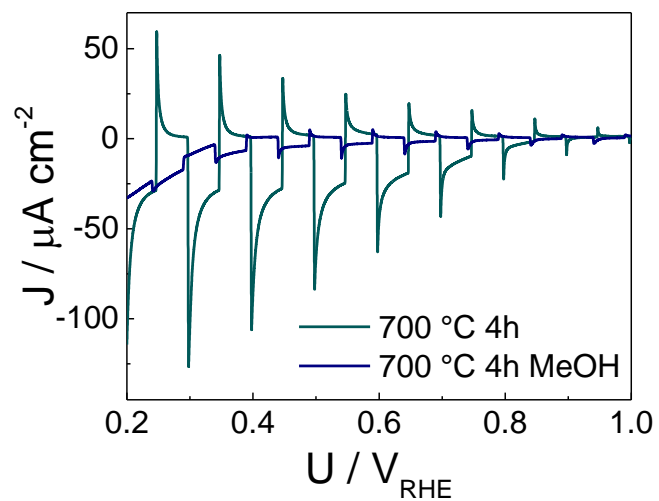


Figure S9. Photocurrent density of a CaFe_2O_4 photoelectrode calcined for 4 hours measured under intermittent irradiation in 0.1 M Na_2SO_4 in the absence and presence of methanol (hole scavenger).

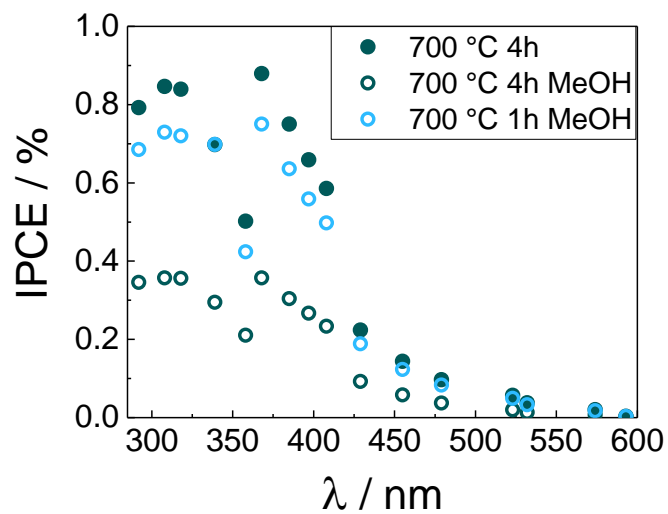


Figure S10. IPCE of a CaFe_2O_4 photoelectrode calcined for 4 hours measured under intermittent irradiation in 0.1 M Na_2SO_4 in the absence and presence of methanol (hole scavenger); for comparison, the IPCE of a photoelectrode calcined for 1 hour in the presence of methanol is shown.

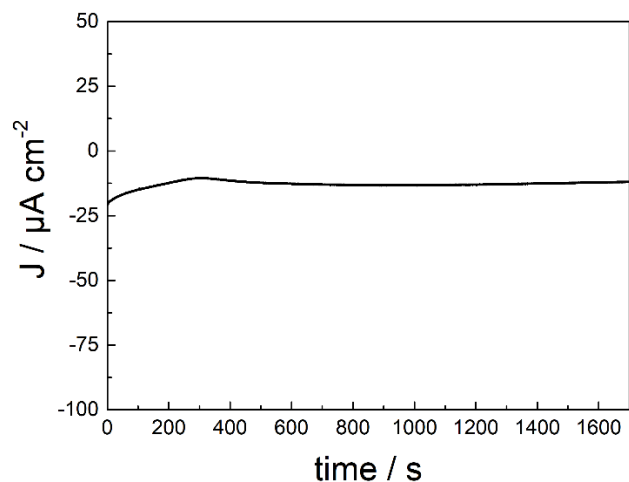


Figure S11. Chronoamperometry of a porous CaFe_2O_4 photoelectrode (calcined at 700°C for 1 hour), measured in $0.1\text{M Na}_2\text{SO}_4$ at $0.3\text{ V}_{\text{RHE}}$ under 1 sun illumination.

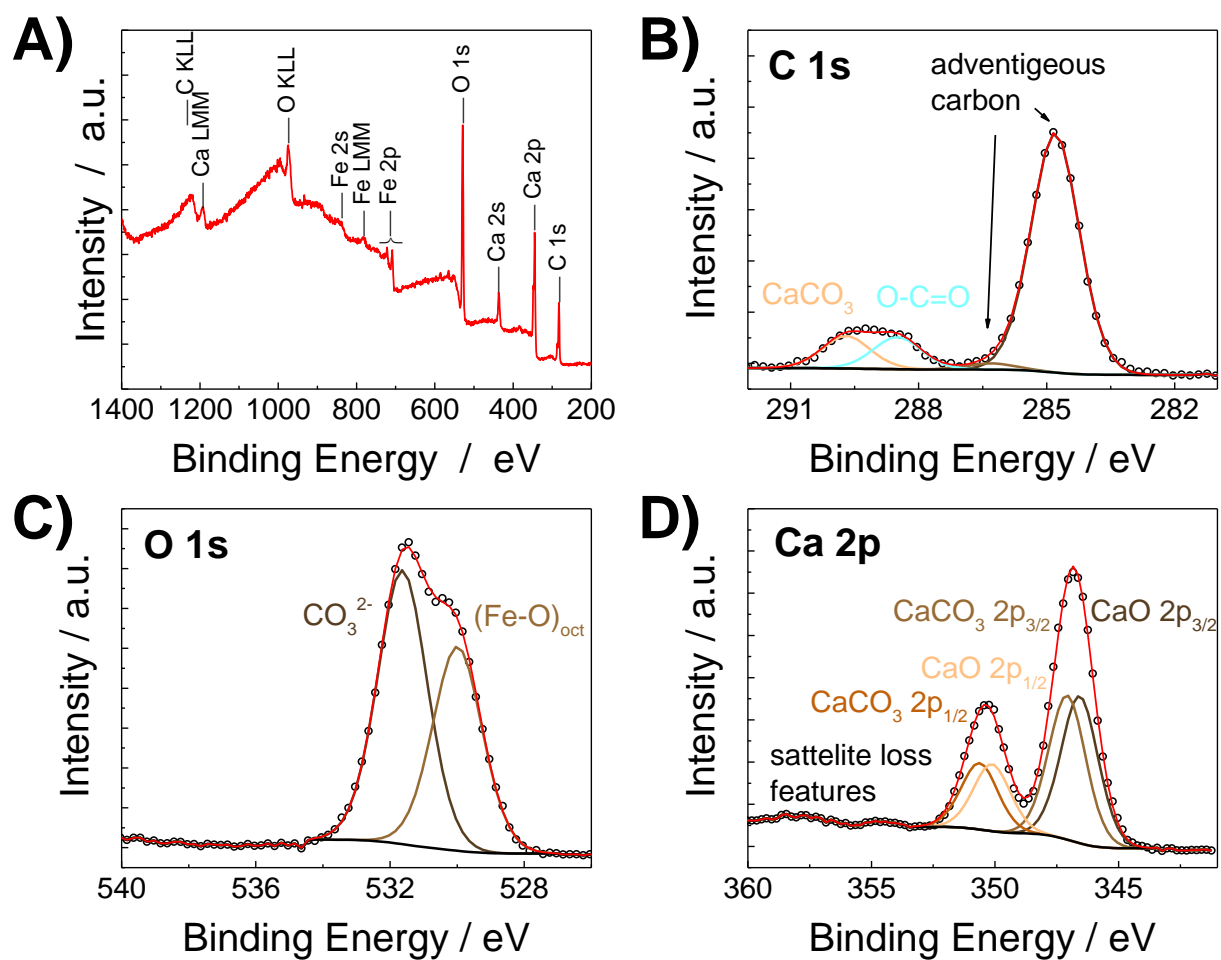


Figure S12. (A) XPS survey and (B-D) detailed spectra for porous CaFe_2O_4 photoelectrode.

C 1s spectra revealed the presence of calcium carbonate (289.7 eV) and carbonate-like (288.5 eV) species at the thin film surface.² This was validated by analysis of the O 1s spectra, which show a CaCO₃ signal at 531.3 eV in addition to the typical Fe-O signal at 529.5 eV reported for octahedrally coordinated iron oxides.^{9,10} The Ca 2p spectra showed a spin-orbit splitting of 3.5 eV, which matches calcium with an oxidation state of +2. Signals for Ca-O bonding at 350.1 eV (2p_{1/2}) and 346.6 eV (2p_{3/2}) were found as well as signals at 350.6 eV (2p_{1/2}) and 347.1 eV (2p_{3/2}) typical for CaCO₃.¹¹ As CaCO₃ has a very low formation enthalpy, the appearance of CaCO₃ during calcination in air is not avoidable.

- (1) Kirchberg, K.; Wang, S.; Wang, L.; Marschall, R. *ChemPhysChem* **2018**, *19* (18), 2313–2320.
- (2) Miller, D. J.; Biesinger, M. C.; McIntyre, N. S. *Surf. Interface Anal.* **2002**, *33* (4), 299–305.
- (3) Bhingardive, V.; Woldu, T.; Biswas, S.; Kar, G. P.; Thomas, S.; Kalarikkal, N.; Bose, S. *ChemistrySelect* **2016**, *1* (15), 4747–4752.
- (4) Ida, S.; Kearney, K.; Futagami, T.; Hagiwara, H.; Sakai, T.; Watanabe, M.; Rockett, A.; Ishihara, T. *Sustain. Energy Fuels* **2017**, *1* (2), 280–287.
- (5) Dotan, H.; Sivula, K.; Grätzel, M.; Rothschild, A.; Warren, S. C. *Energy Environ. Sci.* **2011**, *4* (3), 958–964.
- (6) Li, Z.; Luo, W.; Zhang, M.; Feng, J.; Zou, Z. *Energy Environ. Sci.* **2013**, *6* (2), 347–370.
- (7) Kolev, N.; Iliev, M. N.; Popov, V. N.; Gospodinov, M. *Solid State Commun.* **2003**, *128* (4), 153–155.
- (8) Piovano, A.; Ceretti, M.; Johnson, M. R.; Agostini, G.; Paulus, W.; Lamberti, C. *J. Phys. Condens. Matter* **2015**, *27* (22), 225403 1-11.
- (9) Biesinger, M. C.; Payne, B. P.; Grosvenor, A. P.; Lau, L. W. M.; Gerson, A. R.; Smart, R. S. C. *Appl. Surf. Sci.* **2011**, *257* (7), 2717–2730.
- (10) Baer, D. R.; Blanchard, D. L.; Engelhard, M. H.; Zachara, J. M. *Surf. Interface Anal.* **1991**, *17* (1), 25–30.
- (11) Demri, B.; Muster, D. *J. Mater. Process. Technol.* **1995**, *55* (3–4), 311–314.